01 Mar 1989

Condensation Coefficient Measurement for Water in the UMR Cloud Simulation Chamber

Donald E. Hagen
Missouri University of Science and Technology, hagen@mst.edu

John L. Schmitt
Missouri University of Science and Technology

Max B. Trueblood
Missouri University of Science and Technology, trueblud@mst.edu

John C. Carstens
Missouri University of Science and Technology, carstens@mst.edu

et. al. For a complete list of authors, see https://scholarsmine.mst.edu/phys_facwork/255

Recommended Citation

D. E. Hagen et al., "Condensation Coefficient Measurement for Water in the UMR Cloud Simulation Chamber," *Journal of the Atmospheric Sciences*, vol. 46, no. 6, pp. 803-816, American Meteorological Society, Mar 1989.
The definitive version is available at https://doi.org/10.1175/1520-0469(1989)046<0803:CCMFWI>2.0.CO;2

Condensation Coefficient Measurement for Water in the UMR Cloud Simulation Chamber

D. E. HAGEN, J. SCHMITT, M. TRUEBLOOD, AND J. CARSTENS

*Department of Physics and Graduate Center for Cloud Physics Research**

D. R. WHITE

*Department of Engineering Mechanics and Graduate Center for Cloud Physics Research**

D. J. ALOFS

*Department of Mechanical Engineering and Graduate Center for Cloud Physics Research**

(Manuscript received 29 April 1988, in final form 29 August 1988)

ABSTRACT

A systematic series of condensation coefficient measurements of water have been made using the University of Missouri—Rolla cooled-wall expansion chamber which simulates the thermodynamics of cloud. This coefficient is seen to decrease from a value near unity, at the outset of simulation, to a value in the neighborhood of 0.01 toward the end of a simulation. Final values of this coefficient are sufficiently low as to contribute significantly to the broadening of the drop-size distribution in cloud.

1. Introduction

The breadth of the size distribution of cloud drops remains an issue that has not been completely resolved. The size spectrum of drops grown by condensation is usually regarded as a significant attribute of a cloud, especially in its stability against precipitation (e.g., Paluch and Knight 1986). As is well known, the spread in drop sizes is generally found to be broader than that predicted by closed parcel theory. The broadened distribution is commonly attributed to mixing processes, and a few descriptions of such processes have been suggested (Paluch and Knight 1986; Blyth and Latham 1985; Baker et al. 1984; Telford and Wagner 1981; Telford and Chai 1980; Mason and Jonas 1974). However, although entrainment undoubtedly plays an important role, there is some evidence that it may not tell the whole story, for considerable broadening has been observed even when buoyant parcels remain undiluted. In their observational study of cloud drop spectra in continental cumulus, Jensen and Baker (1986) observe that, in parcels undiluted by mixing, "mean droplet spectra are much wider than those predicted by simple adiabatic parcel models." However some observations have yielded spectral widths as narrow as that given by adiabatic parcel models (Jensen et al. 1985). Paluch and Knight (1986) refer to broadening in closed parcels, suggesting that "there may exist a spectral broadening process not related to mixing"; the same authors (1987) have reminded us that one can hardly attribute broadening to entrainment where it appears that little or no entrainment has occurred. Also we must point out the possibility that some droplet spectrum broadening observed with FSSP (PMS Forward Scattering Spectrometer Probe) sensors may be due to instrumental error (Cerni 1983; Baumgardner 1988).

It is known (Warner 1969) that a "low" condensation coefficient for water can account for observed broadening, or at least that part of it extending toward the smaller end of the drop size spectrum (see also Manton and Warner 1982). Indeed Warner states that a value of 0.014 would be needed (Chodes et al. 1974) to secure agreement between observed and theoretically derived distributions. Chodes et al. (1974) measured a value of 0.033, too large to account for observed broadening, but it should be pointed out that Garnier et al. (1987), who themselves measure a value of .01, have reanalyzed Chodes et al.'s experiment and suggest that the correct value measured in these experiments is "closer to 0.02."

If we assume perfect thermal accommodation (coefficient of unity) the following criteria give a rough idea of the significance of the condensation coefficient, β: if $0.1 > \beta > 0.02$, it is a non-negligible factor in cloud drop condensation; if $\beta < 0.02$, its influence may well

* University of Missouri—Rolla, Missouri.

Corresponding author address: Dr. Donald E. Hagen, Graduate Center for Cloud Physics Research, University of Missouri—Rolla, 108 Norwood Hall, Rolla, Missouri 65401-0249.

be decisive in controlling the spread of the droplet size distribution. Values used in the cloud physics literature often lie in the range 0.03 to 0.036—a choice that appears to be based either on the measurements of Chodes et al. (1974) or on the recommendation of Pruppacher and Klett (1978) on the grounds that 0.035 represents an average for "non-renewed" water surface. It is debatable whether such a choice represents a consensus. Jonas and Mason (1982) point out that the value of the condensation coefficient has "not been reliably determined." In addition to the aforementioned table of Pruppacher and Klett, exhibiting values ranging from 1 to 0.006, other reviewers have likewise tabulated a scattershot of measured values (Maa 1983; Barnes 1978; Mills and Seban 1967; Mozurkewich 1986). There is a consensus that the coefficient should be unity for a pure surface (e.g., Cammenga 1980; Mozurkewich 1986), although Mozurkewich allows that "theoretical estimation of condensation coefficients is not well developed," and that lower coefficients, if they are not due to outright experimental errors, may well be due to contamination (for example, see Bigg 1986). Two sources of error are identified in the literature (e.g., Cammenga 1980; Mozurkewich 1986; Bigg 1986): 1) uncertainty in the measurement of surface temperature and 2) the effect of contaminants. In this experiment the use of unsuspended drops, rather than bulk samples, obviates the first problem. The role of contaminants on our results will be discussed in section 4.

It should be mentioned that the role of the condensation coefficient is similar to that of the thermal accommodation coefficient in influencing drop growth/evaporation, the former affecting mass flux and the latter the thermal flux brought about by the release of latent heat of condensation. In the conventional theory of drop growth, both coefficients enter into the formalism by means of a single (length) parameter (Carstens 1979; Mozurkewich 1986). Measurement of this parameter for a given set of ambient conditions cannot therefore fix both coefficients, but only establish a one-to-one relationship between them (i.e., a continuum of pairs of values). In what follows we have provisionally chosen the thermal accommodation coefficient to be unity so as to secure a particular (and commonly understood) value of the condensation coefficient corresponding to a given measurement. In our measurements we have deliberately established in-cloud conditions corresponding to the continuum regime of droplet growth. Thus, we have not taken advantage of the fact that these coefficients tend to be more rate influencing and hence more readily inferred, in the transition regime (Carstens 1979). On the other hand, except for relatively minor points discussed below, the continuum theory is generally agreed-upon and (except for the value of thermal and/or mass accommodation coefficients) regarded as correct; there is as yet no such unanimity regarding the theory in the transition regime. Moreover, in these measurements we focus on the possibility of "low," that is meteorologically significant, values of the condensation coefficient whose influence extends into the continuum regime. We have in any case taken care to simulate in-cloud conditions with sufficient accuracy that minor rate influencing factors can be sorted out.

2. Theory of drop growth in the continuum

The theory of cloud drop growth by condensation commonly employed by meteorologists has been presented by Fitzgerald (1970) and Fukuta and Walter (1970), among others. It has been elaborated in rather more detail in a number of recent reviews (e.g., Davis 1983; Wagner 1982; Anderson et al. 1981; Carstens 1979) to which we refer for a fuller exposition. Here we adapt the formalism appropriate to the continuum regime following Carstens (1979), and adapted specifically to chamber conditions. This theory appeals to a number of commonly accepted assumptions, which are discussed by Wagner (1982) and Carstens (1979): (i) the drop is assumed isolated from its neighbors, so that the surrounding vapor and temperature fields are spherically symmetric; (ii) quasi-steady state flow of heat and mass is assumed; (iii) the effect of drop fall on growth/evaporation is neglected; and (iv) the effects of thermal diffusion and its inverse (cross terms) are neglected.

Based on Fick's law for a nonisothermal system (Bird et al. 1960), a solution for drop growth (neglecting Stefan flow) may be written

$$\frac{da^2}{dt} = \frac{2M_v n(T_a)}{\rho_l} \frac{D(e_\infty - e_a)}{p} \tag{1}$$

where all symbols are defined in appendix A. The vapor pressure in the gas at $r = a$ is inferred as follows. The relation between e_a and $e_{eq}(T_d)$ is obtained by equating diffusive (conductive) fluxes with the corresponding fluxes calculated from kinetic theory.

$$e_a - e_{eq}(T_d) = \frac{l_\beta}{a}(e_\infty - e_a) \tag{2}$$

$$T_a - T_d \approx \frac{l_\alpha}{a}(T_\infty - T_a) \tag{3}$$

where

$$l_\beta = \frac{1 - \beta/2}{\beta} \frac{4D}{\bar{v}(T_a)} \tag{4}$$

$$l_\alpha = \frac{1 - \alpha/2}{\alpha} \frac{\gamma - 1}{\gamma + 1} \frac{16K}{n(T_a)\bar{v}_g(T_a)R} \tag{5}$$

The drop temperature, T_d, and the corresponding saturation vapor pressure $e_{eq}(T_d)$ may be eliminated from the formalism by appealing to: (i) the energy balance at $r = a$,

$$-\frac{LM_v n(T_a)}{p} D \left.\frac{\partial e(r)}{\partial r}\right|_a = K \left.\frac{\partial T}{\partial r}\right|_a \quad (6)$$

which results in

$$e_{eq}(T_d) - e_\infty = \frac{Kp}{LM_v Dn(T_a)} (T_\infty - T_a); \quad (7)$$

and (ii) the equilibrium relation $e_{eq}(T_d)$. For very low supersaturations, as prevail in atmospheric cloud, the expression $e_{eq}(T_d)$ is often linearized around T_∞ and extended to T_d, i.e.,

$$e_{eq}(T_d) = BT_d + C \quad (8)$$

where B and C are evaluated at T_∞. For higher supersaturations, as achieved by expansion chambers, a more accurate expression for $e_{eq}(T_d)$ must be used. We have retained a similar formalism in both cases by simply linearizing $e_{eq}(T_d)$ around T_d.

Thus, both the conventional low supersaturation case and the high supersaturation case are expressed by the following growth formulation

$$(a + l)\frac{da}{dt} = \frac{\rho_{eq}(T_\infty)}{\rho_l} D_{eff}\left[S - \frac{BT_\infty + C}{e_{eq}(T_\infty)} S_{sat}(a)\right] \quad (9)$$

where B and C are evaluated explicitly at T_d for the high supersaturation case. Here $S_{sat}(a)$ represents the conventional Kohler result (e.g., Fletcher 1962)

$$S_{sat}(a) = 1 + \frac{r^*}{a} - \frac{Am_s}{a^3}, \quad (10)$$

$$\frac{1}{D_{eff}} = \frac{1}{D} + \frac{Bn(T_a)L(T_a)M_v}{Kp} \quad (11)$$

$$l = \left(\frac{l_\beta}{D} + \frac{BLM_v n(T_a)}{Kp} l_\alpha\right) D_{eff}. \quad (12)$$

The parameter r^* is the characteristic Kelvin radius, and A is a constant based on the assumed applicability of Raolt's law to the solute of mass, m_s. We have dropped the Stefan flow correction. [D in Eq. (11) is inversely proportional to p and this pressure dependence is taken into account.]

Finally it should be noted that the expression for l_α exceeds that of Carstens (1979) by a factor of two (see appendix B). For $\alpha = 1$, as is usually assumed, the error in l_α has little effect in the continuum regime. For "low" values of α a factor of two can be significant.

3. Experiment

a. Overview

The experiment is performed in the cooled-wall expansion type cloud simulation chamber (White et al. 1987). A monodispersed cloud (all drops the same size) is formed on a monodisperse NaCl aerosol which serves as the cloud condensation nuclei. The cloud forms when the sample of moist aerosol laden air experiences a supersaturation due to a controlled isentropic expansion. Further cloud growth or evaporation is induced through further expansion or compression. The cloud drop size as a function of time is measured. The corresponding droplet growth rate is compared with growth theory to evaluate a condensation coefficient, β. Two different types of profiles are employed: (i) a "ramp" profile in which a 10°C/min cooling rate (corresponding to a 17 m s^{-1} updraft velocity) is initiated and then held constant; and (ii) an "oscillating" profile produced by a series of expansion/compressions which repeatedly form and then evaporate the cloud. A ramp expansion produces an especially well controlled temperature and pressure profile which allows the tracking of droplet growth to large drop sizes (about 12 μm radius). An oscillating expansion allows repeated drop growth measurements on the same sample of droplets, for the study of memory effects.

b. Monodispersed clouds

The reason for using a monodispersed cloud is the need to make precise drop size versus time measurements. The results from monodispersed clouds can be combined to simulate any polydispersed system, and one can readily measure the size of drops in a monodispersed system. The method for this latter measurement is to observe the characteristic Mie theory maxima and minima of light scattering from the cloud droplets. This technique does not permit us to *directly* observe size spectrum evolution for polydisperse clouds, but involves *all* the relevant physics of the cloud-growth process in the condensation regime. Both chamber and atmospheric drop populations are always sufficiently low that the only "interaction" among drops takes place through their commonly experienced (ambient) vapor pressure and temperature fields, where each growing drop contributes to a uniform decrease in ambient supersaturation. All of the physics is tied up in the droplet growth rate as a function of drop size, temperature, pressure, and supersaturation. Once this is known from monodisperse experiments, the condensational behavior of polydisperse clouds can be accurately predicted.

Monodispersed clouds are obtained by starting with a monodispersed aerosol (NaCl) and subjecting the sample to a fast expansion when the saturation is near 100%. When this is done, all of the CCN activate at about the same time and grow in a similar manner. Our aerosol system produces a quite monodispersed aerosol through the use of an aerosol generator consisting of four furnaces (White et al. 1987; Alofs et al. 1979) followed by electric mobility size classification. The geometric standard deviation of the aerosol size distribution is usually 10% of the mean size. All of our

experiments are designed such that the expansion rate was 10°C min^{-1} when the sample reached 100% relative humidity, i.e., the supersaturation ratio (S) reached unity. During subsequent growth, the droplet size distribution becomes more monodispersed since, as is well known, diffusively controlled condensational growth naturally sharpens the size distribution. We estimate from the sharpness of the Mie scattering peaks (see below) that the drops are routinely monodispersed to within 0.1 μm.

c. Introduction of the aerosol

The aerosol is introduced into the middle of the flow of clean moist air supplied by the humidifier system. The ratio of humid air flow to aerosol air flow is adjusted to produce an aerosol concentration in the simulation chamber between 25 and 150 particles per cubic centimeter. This ratio is always kept at values greater than 100:1 so that uncertainties in the relative humidity of the aerosol air stream will not interfere with our ability to set the total sample relative humidity to a desired value. The aerosol concentration in the simulation chamber during the flushing period is determined by withdrawing a continuous sample from the chamber and measuring the total aerosol concentration with the alternate gradient continuous flow diffusion chamber (AGCFD). This chamber is similar to that described by Hoppel et al. (1979).

The chamber is flushed with a sample flow from top to bottom for at least 15 minutes and until a stable, usable aerosol concentration is measured for 5 minutes. At that time the appropriate (for the measured aerosol concentration) computer control profile is selected for use and the chamber inlet and outlet valves closed. Once the inlet and outlet valves are closed the pressure control is activated and a slow isothermal compression or expansion brings the chamber to the required starting pressure of 972.2 mb. The wall temperature control has been operating before the sample flush and holds the walls constant at the desired initial temperature. Loss of CCN aerosol to the chamber walls during the stilling period after closing the chamber has been estimated using the aerosol diffusive deposition theory developed by Pich (1976) and was found to be negligible.

d. Preparation of humidified air

Air for the experiments is taken from outside the laboratory building at a flow rate of approximately 1 L s^{-1}. The air is dried by both refrigeration and desiccant driers and filtered with both particle and activated charcoal filters (White et al. 1987). The resulting clean dry air is then passed through a precision flowing water humidifier (White et al. 1987; Hagen et al. 1988) to establish a known water vapor content. The aerosol is then added at the output of the humidifier.

e. Humidity measurement

The relative humidity in the simulation chamber prior to expansion is a key parameter in virtually any experiment since it controls the humidity at all later points in the experiment. In this work the cloud chamber itself is used as a condensation type hygrometer to calibrate the humidifier to a precision of one part per thousand in mixing ratio (Hagen et al. 1988). Two distinct methods are employed. One is based on repeated measurements of droplet growth rate during the course of an experiment; the other is based on the fact that cloud is observable almost immediately after the gas sample is brought through 100% relative humidity. In the former method the influence of the condensation coefficient is eliminated by using the fact that the initial mixing ratio is a constant. In the latter method the condensation coefficient enters only as a minor correction. The two methods agree well. The average difference in calculated initial mixing ratio is 1×10^{-5} grams of water per gram of dry air (corresponding to about 8 parts in 10^4), with a standard deviation of 0.7×10^{-5} grams/gram-air. This corresponds to a dewpoint difference of 0.012°C at 17°C. This is a state-of-the-art humidity measurement. For comparison, the manufacturer's claimed accuracy for a commercial humidity measurement device, the Cambridge Systems dewpoint hygrometer model 992, is about plus or minus 0.55°C. As will be discussed later, our small uncertainty in mixing ratio does lead to the largest experimental uncertainty in the condensation coefficient.

f. Cloud observations: Motion in the viewing volume

Conditions in the central volume of the simulation chamber are monitored using a low light level video camera capable of detecting individual drops with radii of 2.5 μm and larger. Illumination is provided by the same laser beam used for the 4° forward Mie scattering system, which also measures the average drop radius as a function of time. The video camera is located at the chamber window at 72° from the forward direction of the laser beam and views a horizontal cylindrical volume in the center of the chamber approximately 2 cm in diameter and 6 cm long. The volume observed by the video camera and the Mie scattering volume are approximately coincident.

Visual observation of the clouds shows the droplets to be either stationary or moving together (1 to 2 cm s^{-1}) in a uniform, organized manner during the time interval for which Mie scattering data can be interpreted. Experience has shown that the degree to which the cloud droplets are stationary is closely related to the accuracy with which the computer control profile matches the actual chamber conditions. The gas and wall temperatures must be matched to better than a tenth of a degree Centigrade in order to suppress convection. Gas pressure and temperature control profiles are calculated in advance of the experiment using Hag-

en's numerical cloud model (Hagen 1979). Since the condensation coefficient, β, exerts some control over the release of latent heat of condensation, which largely determines the temperature, a good knowledge of β is a prerequisite for performing the experiment. We accomplished the task of measuring β in an experiment in which a knowledge of β was a prerequisite, by repeating the experiment many times. At each repetition our knowledge of β improved, and with it, chamber control. Since the influence of β enters into the control scheme only through latent heat release, its influence is felt only towards the latter part of the experiment when the drops are several microns in size. During the early experiments our knowledge of β was relatively poor, and convection interfered with the measurements. As our knowledge of β improved, convection could be suppressed longer, and measurements could be extended to larger drop sizes. The results shown here are based on our best estimates of β, which did prove sufficient to suppress convection. The suppression of convection gives evidence that our cloud model, using the condensation coefficient shown here, did satisfactorily track the growth of the cloud drops.

g. *Measurement of drop radius versus time*

The size of the drops as a function of time are measured by analysis of Mie light scattering at 4° from the forward direction. Details of the simulation chamber optics system along with a diagram have been given by White et al. (1987). Illumination for the 4° Mie scattering system is provided by the beam-expanded 488 nm line of an argon-ion CW laser. The beam is expanded to a diameter of approximately 1.5 cm and enters through one of the three chamber windows. As the beam enters the chamber it passes through an optical wedge which deflects it upward at an angle of 2°. The photomultiplier tube detector views the center of the chamber through an identical optical wedge, located in the chamber window directly opposite the laser entrance window, which deflects its viewing direction upward by 2°. This results in the photomultiplier tube receiving light which has been scattered at approximately 4° from the forward direction by a small volume (about 30 cm^3) of droplets in the center of the simulation chamber. A pinhole aperture in front of a photomultiplier tube restricts the acceptance angle of scattered light to a 1° viewing angle which intersects the laser beam in the center of the chamber.

The output of the photomultiplier tube is amplified and recorded on a photographic paper oscillograph (d.c. to 5 KHz response). Prior to the beginning of the cloud formation, but after the recorder has started, a computer controlled shutter is closed in front of the photomultiplier tube to provide an absolute correlation between the recorder time and the computer time. A second recorder channel records a bilevel signal, which changes state with each update of the pressure control system. The computer also records the times of each pressure control update and these times together with the shutter time are used to synchronize the recorder trace with the computer time.

h. *Light beam recorder trace analysis*

A plot of the Mie scattering intensity as a function of droplet size for scattering angles around 4° provides a very distinct system of peaks and valleys. A sample scattering intensity vs. droplet size plot is shown in Fig. 1. Correlation of droplet size and scattering intensity was made only for the local maxima and minima of the recorded intensity vs. time trace.

Computer computations of the scattering intensity versus droplet radius have been plotted for scattering angles between 3.0° and 5.0° at 0.25° intervals. The intensity was integrated over a 1° acceptance angle to duplicate the optics of the photomultiplier tube. Study of these plots show local extrema with frequencies of 2 to 4 per micron of droplet radius with a slower modulation of the maxima with a period of 3 to 4 micron.

Once the scattering angle has been determined the appropriate computer generated plot is used to determine the corresponding droplet radius for each of the local extrema. The light beam recorder trace combined with the computer recorded time of the shutter closing (which produces a very distinct offset in the trace when the background light is cut off) is used to establish an absolute time on the trace. From there the time of the next pressure update trace state change is determined and the times of succeeding state changes are determined by making a one to one correlation between state changes and the computer recorded pressure update times. By interpolation between known times on the trace the corresponding computer time is determined for each of the local extrema of the scattering intensity trace.

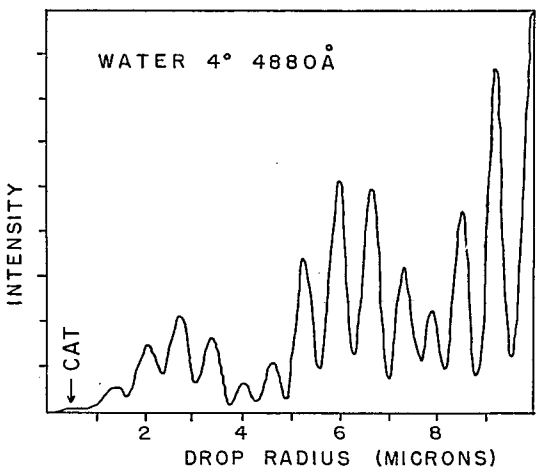

FIG. 1. Light scattering intensity vs drop radius as calculated via Mie theory for water at 4° from the forward scattering angle. CAT denotes the point in time at which the cloud is first observable.

i. Theoretical relations used to determine condensation coefficient

Condensational droplet growth theory as developed by Carstens (1979) and discussed by Hagen (1979) is used in the analysis of this data. In this analysis we invoke the usual assumption that the thermal accommodation coefficient is unity, and the condensation coefficient (β) is the only experimental unknown. Two different implementations of the theory are employed depending on whether or not the driving supersaturation is high enough to lead to a significant difference between the ambient gas temperature and the cloud drop temperature.

For experiments in the cloud simulation chamber, all of which are done at relatively low supersaturations (usually the maximum supersaturation is around 5 or 6%), the difference between the ambient temperature and that of the drop is slight enough that the saturation vapor pressure may be inferred, with acceptable accuracy, by a linear fit spanning these two temperatures. For this simple case, the droplet growth theory can be algebraically inverted to give β as a function of growth rate:

$$\beta = 2 \Big/ \left\{ 1 + \frac{\bar{v}}{2(1-\bar{e}/p)} \left[\frac{\rho_{eq}}{\rho_l} \frac{S - S_{sat}(a)}{\dot{a}} - \frac{a}{D_{eff}} - \frac{BLM_v n(T_d)}{pK} l_\alpha \right] \right\}. \quad (13)$$

For the case of high supersaturations such as those encountered in the piston-driven fast expansion chambers, the linearization technique (valid for low, in-cloud, supersaturations) must be abandoned. Here the inversion of the droplet growth equations to find β cannot be done algebraically due to the dependence of the drop temperature on β. The inversion must be done numerically. The first step is the calculation of drop temperature, T_d, from the Eqs. (1)–(8). Then $\dot{a}$ is given by Eq. (9). The resultant β is the one which makes $\dot{a}$ equal the measured growth rate.

j. Comparison with other drop growth theories

The model used for our analysis (Carstens 1979) has been successfully tested against older results in the literature (Hagen 1979) and against the NASA Analytic Simulator (Plooster 1979). Anderson et al. (1981) presented an extended solution to the droplet growth problem and intercompared the leading droplet theories. They concluded that Carsten's (1979) solution of the droplet growth problem produced valid results. This is the solution on which our cloud model is based. Furthermore Anderson et al. (1981) presented numerical results from their extended model for numerous test cases. We recalculated these cases with our model and agree with their results to within 2% for drop size. Note that in this application only the differential form of droplet growth theory is used. Theory is also used to provide a value for the instantaneous growth rate for a given environmental condition (temperature, pressure, and supersaturation). Integration of the droplet growth equations over time, as is done in a full cloud model, is not required or used here.

k. Determination of temperature, pressure, and supersaturation

In this condensation coefficient analysis there is no integration of droplet growth equations, since the drop size $a(t)$ is directly measured via Mie light scattering. The pressure $p(t)$ is also directly measured via a wide bandwidth pressure transducer. The temperature $T(t)$ is calculated from the first law of thermodynamics, assuming an isentropic expansion, from the measured $p(t)$ and $a(t)$ profiles and the initial value of temperature, T_0. From these measured parameters, the supersaturation can be directly calculated (Hagen 1979):

$$S = \frac{p}{e_{eq}(T)} \frac{1}{1 + \frac{\epsilon}{r}}$$

where r denotes the current mixing ratio as determined from the initial mixing ratio, drop concentration and current drop size.

l. Temperature and pressure profiles

Figure 2 shows the temperature and pressure as functions of time profiles for a ramp expansion. After a short start-up period the temperature falls at a constant rate of 10°C min^{-1}. With this profile the cloud forms, its growth is observed, and the experiment ends when control prediction errors lead to a temperature mismatch between the gas and walls which induces cloud nonuniformities and convection. Typically the cloud can be measured to a size of 12 to 15 micron radius. Figure 3 shows profiles for an oscillating expansion. For this latter profile we get cloud formation followed by evaporation for each of the cycles. The last cycle does not turn around into a compression, but rather continues into a standard 10°C min^{-1} ramp. Note that the first cycle is not as deep as the subsequent ones. After experimentation we discovered that the cloud drops grow much more rapidly during the first expansion, and so we reduced its depth to grow the drops to about the same size on each cycle. With this type of expansion profile it is possible to study repeated droplet growth behavior on fresh versus aged cloud drops, using the same CCN-gas sample.

m. Results

Ramp experiments. These use the profiles shown in Fig. 2. In these experiments a number of runs were done on the same day, and the results are superimposed

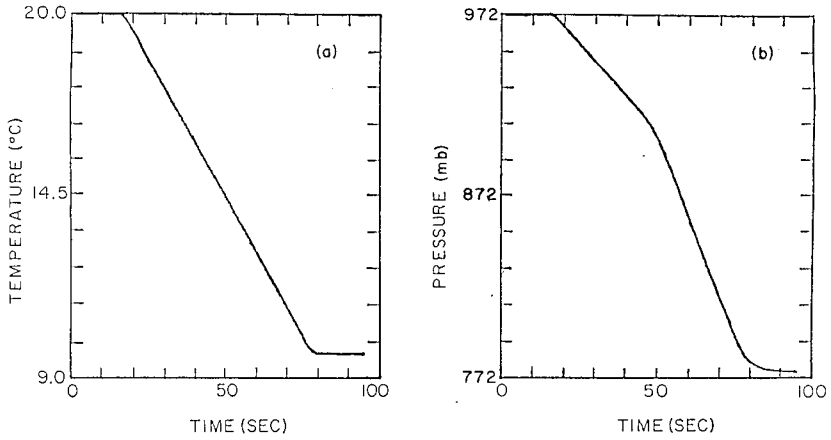

FIG. 2. Expansion chamber temperature (a) and pressure (b) vs time profiles for "ramp" expansions.

on the same graph. In this way experimental noise is averaged out and the trends in the data are most apparent. The condensation coefficient, β, is inferred from measured droplet growth. Because growth can be repeatedly determined throughout the course of the experiment, so too can β be repeatedly determined from each growth rate value. We find that β changes with time. It is found useful to plot β versus droplet size, a, not because we necessarily expect an explicit β versus a dependence, but rather because drop radius reflects the duration of the imposed driving force experienced by the growing drops. Plots for three sets of experiments are shown in Figs. 4–6. Each figure represents a su-

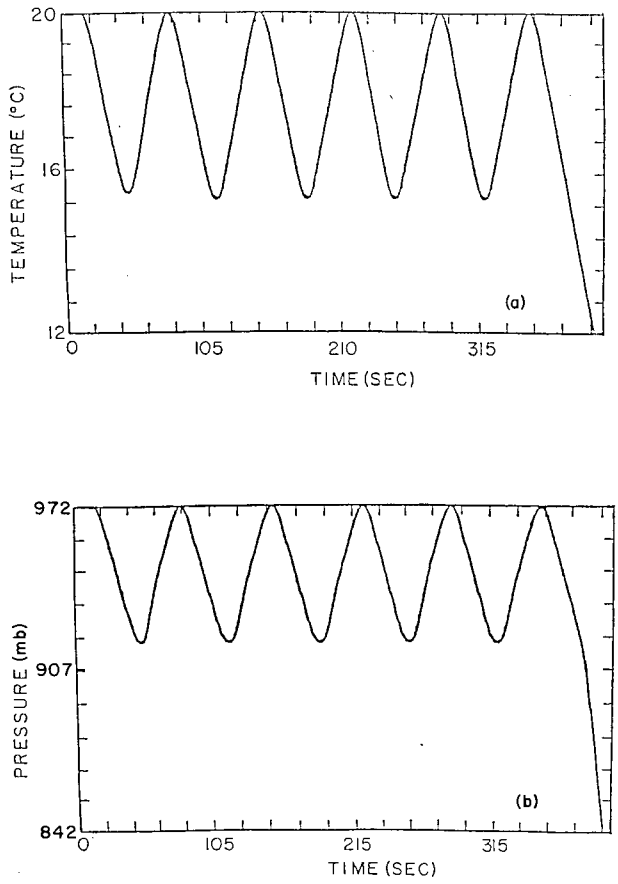

FIG. 3. As in Fig. 2 but for "oscillating" expansions.

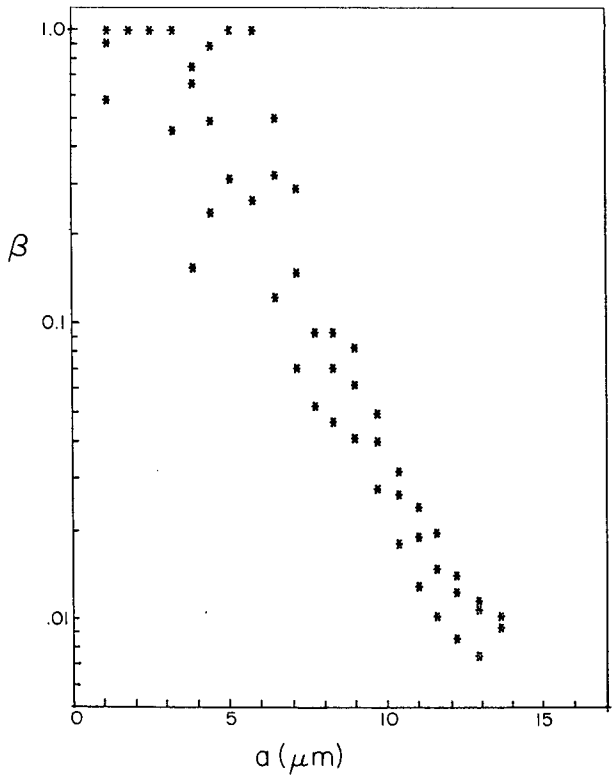

FIG. 4. Superposition of condensation coefficient, β, vs cloud drop size, a, for cloud simulation chamber experiment series 091086.

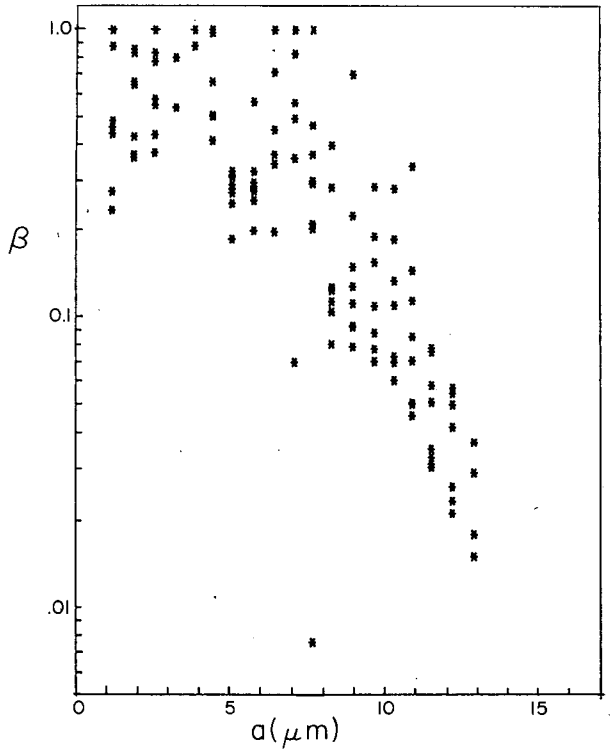

FIG. 5. As in Fig. 4 but for series 121786.

perposition of the results from one day's experiments, using 10°C min^{-1} ramps.

Several features stand out in the graphs. The results at large β exhibit a relatively large amount of scatter. This is a consequence of the fact that when β is large, it has only a small effect on droplet growth. Hence small errors in growth rate translate into very large errors in β. Here β is seen to start out near unity for fresh drops (i.e., drops which have not been previously activated). This is an expected result for pure water drops with fresh surfaces (Pruppacher and Klett 1978; Cammenga 1980). Now as the drop grows (ages) β begins to decrease significantly. Near the end of the experiment β is near 0.01. This is sufficiently small to have significant atmospheric implications. Here we have shown three sets (days) of experiments; numerous other ramp experiment datasets exhibit the same trends. In order to study this process on a different time scale, one series of 5°C min^{-1} ramp experiments was performed. The resulting $\beta(a)$ was found to be very similar to those from 10°C min^{-1} ramp experiments.

Similar experiments were performed in a completely different cloud chamber facility, a piston type expansion cloud chamber. This is a precision device designed especially for work on homogeneous nucleation (Schmitt 1981). Here the expansion is much faster than in the cloud simulation chamber, the cycle lasting only on the order of a few seconds. Droplet growth rate measurements are made for a few seconds following the expansion. Any condensation nuclei can be removed from this chamber by nucleating on them at supersaturations slightly less than that required for homogeneous nucleation (e.g., 400%–500% relative humidity). The subsequent homogeneously nucleated drops are then pure water and their growth is observed via Mie scattering. Results for one typical experiment are shown in Fig. 7, for the growth of homogeneously nucleated water drops in argon. The results are strikingly similar to those from the cloud simulation chamber which operates on a much slower time scale. β starts off near unity and then falls off as the droplet grows.

A major feature of this fast expansion chamber is its cleanliness. The drops are homogeneously nucleated so there is no CCN aerosol required in the system. Chamber surfaces are Teflon, stainless steel, and glass and can be rigorously cleaned. Data were taken with this chamber before and after a thorough cleaning with an extended application of reagent grade acetone followed by vacuum evaporation. The data taken after the cleaning is shown in Fig. 7. The data taken before the cleaning looks similar to that in Fig. 7 but it converges to about $\beta = 0.2$ in the small drop size limit, suggesting that contaminants can indeed lower the value of β. Other drop growth data is available from Wagner (1982), again for homogeneously nucleated

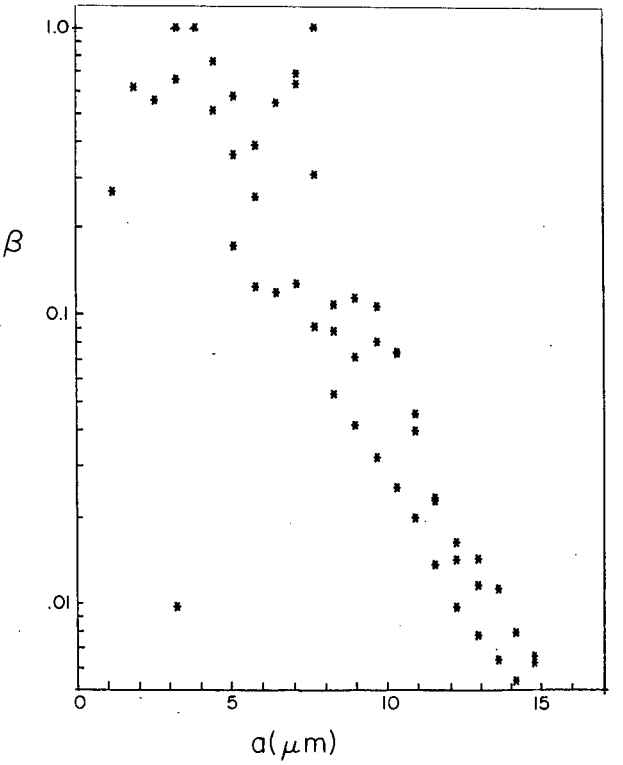

FIG. 6. As in Fig. 4 but for series 111886.

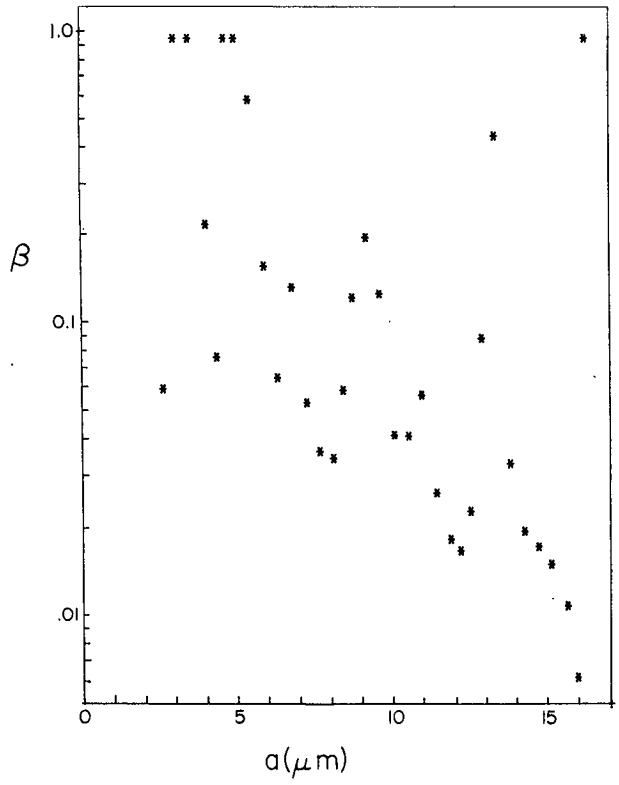

FIG. 7. Condensation coefficient, β, vs cloud drop size, a, for fast piston expansion chamber experiment 121486.

droplets in a high speed piston expansion cloud chamber. This expansion chamber operates on a very short time scale; it is roughly a factor ten faster than the expansion chamber (Schmitt 1981) at the University of Missouri (discussed above). Wagner (1981) presented three experiments. He followed the common approach of fitting one value of β to an entire experiment dataset, rather than allowing it to change its value during the course of an experiment. He found $\beta = 1$ to give the best fit. We reanalyzed the data using our method which gives a β value for each drop size measurement point. In two of his experiments, those with the highest expansion rates and shortest durations, we also find $\beta = 1$ for all points. In the last experiment with the slowest expansion rate and longest duration, we find $\beta = 1$ for the early points, and then found β to fall off reaching $\beta = 0.06$ for the latter points. This indicates that the same trend for β (to begin near unity for fresh drops and then fall off with time) is observed in another completely different cloud chamber system.

Our next experiments are those using the oscillating profiles shown in Fig. 3. Here the sample is subjected to repeated cloud growth and evaporation cycles. Figure 8 shows results for the first two cloud forming stages of a particular oscillating experiment (run 080787.03). These results are typical. The asterisk points show results for the first growth period, and the open-circle points show them for the second growth period. During the first growth period, β starts off near unity and then falls. During the second growth period, β starts off near the β-value where the first expansion left off, and then decreases from there. This behavior is typical and was reported earlier (Hagen 1986). The droplets are "changed" during the first cloud forming experience: their condensation coefficient is lowered, and they do not recover their fresh-drop properties when they are evaporated.

Data for several oscillating experiments are shown in Fig. 9. Nine experiments (separated by vertical dashed lines) are shown. They are taken from two series, 080787 and 100687. The numbers, e.g., 0.03, above the horizontal curly brackets identify a particular run in a series. Recall that these experiments involve a series of cloud growth and evaporation stages. For each stage we have calculated and plotted the average value of β for that stage (the first point depicts the first growth stage, the second point the second growth stage, etc.), and then constructed error bars corresponding to the standard deviation about that average. These error bars reflect the range of values experimentally found. In the calculation the natural logarithm of β rather than β itself was averaged. Individual experiments consist of six or less growth stages.

These data show the following trends. During the

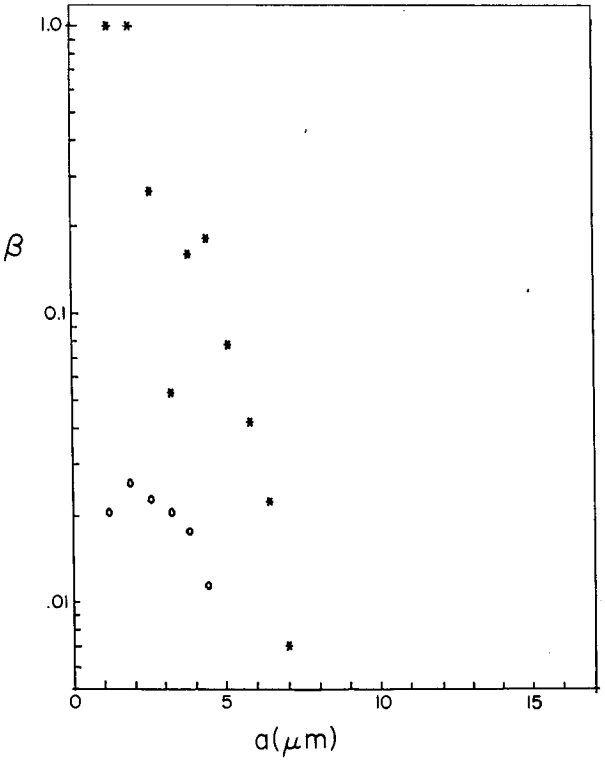

FIG. 8. Condensation coefficient, β, vs. cloud drop size, a, for the first expansion (*) and for the second expansion (O) in the cloud simulation chamber "oscillating type" experiment 080787.

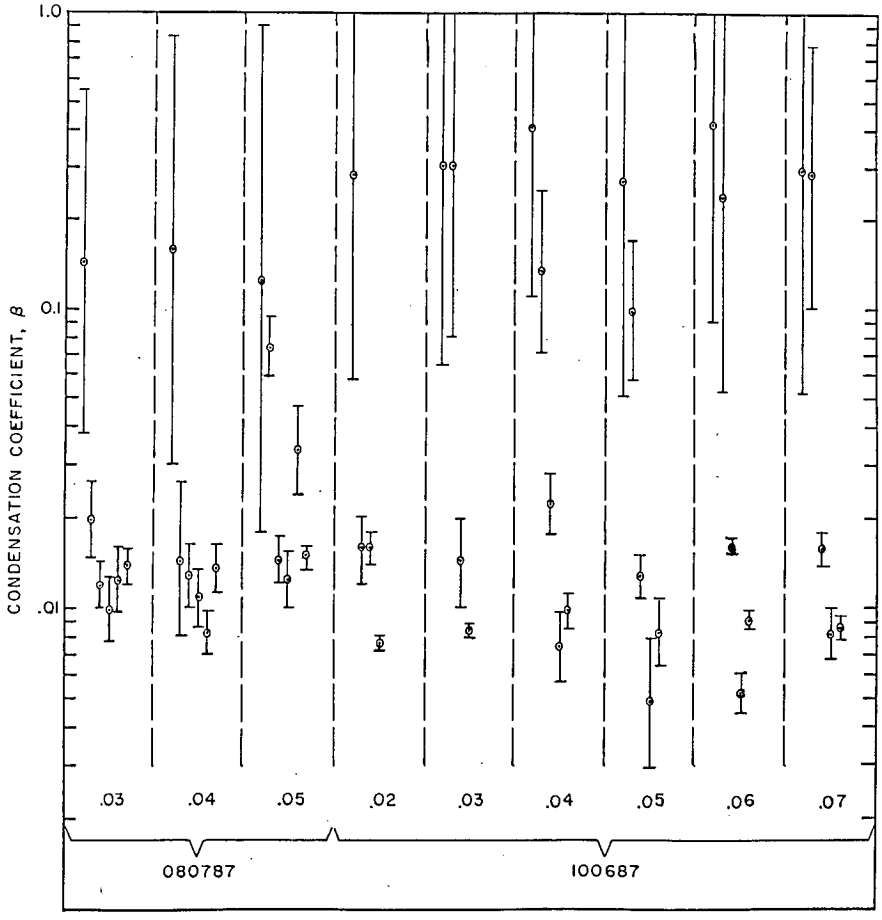

FIG. 9. Condensation coefficients, β, and corresponding error bars resulting from the various cloud drop growth stages of the oscillating-type cloud simulation chamber experiment series 080787 and 100687.

first growth stage the average β is large, typically around 0.2. It exhibits relatively large error bars, and this is due partly to the fact that β is changing substantially during the course of the stage. Subsequent growth stages typically show a much lower β, with an overall average of 0.01, and have much smaller error bars. On some occasions growth stage 2 shows a higher β than the following growth stages, but is usually significantly lower than that for the first growth. Recall that all the growth stages for a given experiment use the same sample of moist aerosol laden air. Growth stages 2 and greater are clearly different than growth 1. In general, most of the β decrease occurs between the first and second growth stages. Even without the benefit of analysis, this effect is evident in the raw data. At similar points in the expansion the cloud droplets are simply growing slower in the subsequent growth stages as compared to first growth. This likewise can be seen in the raw $a(t)$ data. Note that the average β for aged drops is 0.01, which is in a region which makes it sufficiently rate controlling to give β significant atmospheric importance (Chodes et al. 1974).

Some data were taken for the evaporation stages of the experiment. Usually our chamber control is not as good during the evaporation stages of the experiment, and the Mie light scattering traces are noticeably inferior. Data were therefore only analyzed for the first evaporation stage. They showed larger error bars than growth stage 1, and the magnitude of the error bars can be attributed to scatter as opposed to systematic change in β with time. The overall average β for evaporation stage 1 was 0.13, which is between the averages for growth stage 1 and the subsequent growth stages.

n. Error propagation

The major uncertainties in the analysis of β arise from two sources: 1) uncertainty in droplet size (a) measurement, and 2) the uncertainty in the determination of initial water vapor mixing ratio (r_0), which controls the supersaturation. Reasonable error estimates for these variables are $\delta a = 0.025$ μm and $\delta r_0 = 0.000007$ (Hagen et al. 1988). The error in a is random, while the uncertainty in r_0 is systematic.

Numerical analyses were performed using test cases to determine the propagation of these two errors into the final result for β. We found that a random 0.025 μm error in drop size measurement leads to an error in β of 11% for large β (near unity) and of 2% for small β (near 0.03). The $\delta r_0 = 0.000007$ leads to a systematic error in β of 47% for large β and of 7% for small β. Clearly the largest source of uncertainty lies in δr_0, but its contribution is sufficiently small for the data to be meaningful. However, it is clear that accurate humidity measurement is a prerequisite for condensation coefficient measurement studies.

4. Discussion

a. *Contamination hypothesis*

The behavior of β for condensing drops has been an unexpected and perplexing result of these experiments. Although there are many measurements of low coefficients (e.g., Pruppacher and Klett 1978), the consensus appears to be that β should be unity for a pure surface (Mozurkewich 1986; Palmer and Bose 1981; Cammenga 1980; Sherwood et al. 1975; Hickman 1966), and there have been a number of measurements to support this consensus (Schulze and Cammenga 1980; Rubel and Gentry 1985; Wagner 1982; see also Pruppacher and Klett's compilation, 1978). Narasawa and Springer (1975) distinguished between a fresh surface, for which a value near 0.2 was measured, and a "stagnant" surface which exhibited a coefficient of 0.038. The trend of the data reported here are consistent with the conjecture that trace contaminants, probably from the gas, play an important role in the condensation of micron-size drops. Indeed, Cammenga (1980) echoes the concern of other researchers in stating that "most phase transitions, especially evaporation and condensation at liquid surfaces, are extremely sensitive to minute contaminants which are very difficult to exclude." Nor is their effect confined to the phenomenon of condensation: Lucassen-Reynders and Lucassen (1969) have reported substantial damping of water waves by surfactants at well below the concentration needed to form monolayer coverage. Contamination from the soluble (NaCl) aerosol is also a possibility, but it is hard to convince oneself that there could be enough of it to seriously affect growth to large sizes.

The trace contaminant most effective in retarding condensation rates (lowering β) would appear to be surfactants. Their role in retarding hydrometeor growth/evaporation has received considerable attention (Bigg 1986; Toosi and Novakov 1984; Gill et al. 1983; Graedel and Weschler 1981; Garrett 1978; Bullrich and Hanel 1978), and a number of investigations have focused on the extreme retardation associated with complete coverage, (e.g., Rubel and Gentry 1984, 1985; Derjaguin et al. 1966; LaMer 1962). Comparatively few studies have been addressed to analyzing or measuring the effects of partial coverage (Carstens and Podzimek 1986; Rubel and Gentry 1984; Derjaguin et al. 1982; Dickenson 1978). These studies suggest that partial coverage by trace surfactants can affect the magnitude of β although it is hard to justify quantitative estimates of the effect.

In the work described herein we have taken precautions to ensure system and sample purity. Particular care has been taken with the fast expansion chamber both in its construction (all interior surfaces are Teflon, glass, or stainless steel) as well as its cleaning [bake-out at 87.7°C, followed by cleaning with reagent grade acetone, and prolonged spraying of the interior with Burdich and Jackson (1953 S. Harvey St., Muskegon, MI 49442) high purity water].

At this point we are not able to identify (much less monitor) trace contaminants that may remain in these systems after the cleaning process. If it is indeed trace contaminants that cause the decrement in β, observed in both the fast expansion and simulation chambers, it is likely that such levels of contamination exist in real atmospheric conditions as well as in most "normal" laboratory conditions. The identification and quantitative analysis of the contamination would constitute a separate investigation and is not attempted here.

b. *Implications of droplet ageing (contamination)*

A real atmospheric aerosol is likely to be a mixture of fresh and aged particles, including evaporated hydrometeors. The above results imply that the aged component will respond more slowly to imposed high humidity conditions (Bigg 1986). Cloud drop evaporation at a cloud's side boundary or that associated with top mixing by a growing cumulus would be sources of aged aerosol. When aerosol resulting from cloud drop evaporation is mixed with fresh aerosol and reingested into cloud base, the fresh aerosol will have a higher condensation coefficient and will grow faster than the aged aerosol droplets. Hence the fresh aerosol CCN can produce larger drops. Combustion aerosol injected into the atmosphere in large fire plumes can be another source of aged aerosol. A major fraction of such aerosol passes through a nonprecipitating cap cloud which often forms at the top of the fire smoke plume (Radke et al. 1983). The CCN activate, form small drops, and then evaporate. Their subsequent evolution will be as aged aerosol particles and will exhibit the smaller condensation coefficient associated with aged drops. This aging effect will extend their lifetime in the atmosphere.

c. *Thermal accommodation coefficient*

In this analysis the thermal accommodation coefficient has been assumed to be unity. All of the burden for slowing droplet growth has been assigned to the

condensation coefficient. Even though these two coefficients enter into the droplet growth rate via a single length parameter l, they do exhibit different temperature and pressure dependencies, and hence it is feasible to separate them in the analysis by treating data from experiments performed at widely different temperatures and/or pressures (the major disadvantage in reducing pressure, as previously pointed out, is that it brings the transport phenomenon into the transition regime). However, this has not been done here. All of the present experiments were done at about the same temperature (near 16°C) and pressure (near 13 psi). In addition, recent water drop growth measurements (Sageev et al. 1986) on drops held in an electrodynamic balance imply a thermal accommodation coefficient that is near unity, leading to a minimal influence of thermal accommodation on droplet growth.

5. Conclusions

In this study cloud drop growth observations are made under known temperature, pressure, and supersaturation conditions and then analyzed to determine condensation coefficient with the assumption that the thermal accommodation coefficient is unity. The condensation coefficient, β, is found to be near unity for fresh drops. It then falls off with time. Data taken in fast piston expansion cloud chambers, employing vastly different supersaturations and time scales, exhibit trends similar to those found in the cloud simulation chamber. Once a droplet has been aged (and perhaps contaminated) it retains its lower β value even when evaporated, and the lower β is exhibited when it is subsequently subjected to cloud formation and growth. The average β for aged drops is 0.01, as determined from growth cycles two through six in our oscillating profile experiments. This is in agreement with Garnier et al. (1987). The trend of a much smaller β for aged drops cannot in fact just be an artifact associated with the theory or the analysis, because it can be seen in the raw $a(t)$ data. Growth is much slower for aged drops than for fresh drops under the same conditions. A β near 0.01 is sufficiently small to have a significant effect on the broadening of the size distribution of cloud drops in a developing cloud. Moreover a spectra of β values would be a further mechanism for broadening.

6. Raw data availability

The data from the cloud simulation chamber experiments from which the above analysis was done is available to anyone who may wish to subject the data to other models. These data cover 25 simulation chamber experiments: 16 ramp experiments and 9 oscillating experiments.

This data is contained in one ASCII file. The data is available on floppy disk (IBM PC 3.5 or 5.25 inch, DEC RX01/RX02 8 inch), 9-track magnetic tape, and over BITNET from address C3102 @ UMRVMB or over INTERNET/ARPANET from address C3102 @ UMRVMB.UMR.EDU.

Acknowledgments. The authors would like to thank R. Hopkins and M. Alcorn for their work on chamber operations, Drs. Venable, Hanna, and Bertrand for advice on the cleaning of systems, Drs. Salk and Podzimek for useful discussions, and Ms. V. Maples for careful preparation of the manuscript.

This research has been supported by a tri-service grant (AFOSR, ONR, ARO) through AFOSR (85-0071).

APPENDIX A

List of Symbols

English symbols

Symbol	Definition
a	drop radius
$\dot{a}$	time derivative, drop radius
B	slope of (water) saturation vapor pressure curve
D	diffusion coefficient, water vapor in air
e	vapor pressure of water
$e_{eq}(T)$	saturation vapor pressure of water at temperature T
e_∞	vapor pressure of water far from drop (ambient)
e_a	vapor pressure of water at drop surface
$\bar{e}$	$=(e_\infty + e_a)/2$
K	thermal conductivity of air
L	latent heat of condensation of water (cal gm^{-1})
M_a	molecular weight, air
M_v	molecular weight, water
$n(T)$	gas molar concentration at temperature T
N	drop concentration
p	total pressure
R	gas constant
r	mixing ratio or radial variable
r_0	initial mixing ratio
S	supersaturation
S_c	critical supersaturation
T	temperature
T_a	temperature in gas at surface of drop
T_d	drop temperature
T_∞	temperature far from drop (ambient)
$\bar{v}_g(T)$	average speed of gas molecules at temperature T
$\bar{v}(T)$	average speed of vapor molecule at temperature T

Greek symbols

α	thermal accommodation
β	condensation coefficient
γ	ratio of specific heat at constant pressure to that at constant volume (air)
ϵ	ratio of molecular wt. of water to that of air
ρ_s	density of NaCl
ρ_l	density of liquid of which drop is composed
$\rho_{eq}(T)$	equilibrium vapor density at temperature T

APPENDIX B

Kinetically Calculated Thermal Flux

The mass and thermal accommodation coefficients (β and α) may be introduced into the continuum theory by equating the fluxes calculated from uniform gas kinetics to those based on the usual phenomenological laws (Fick and Fourier).

A careful evaluation of the thermal flux term reveals a factor of two that is not present in previous calculations (e.g., Carstens 1979; Fukuta and Walter 1970). In general this has not given rise to serious error, as α has been always set to unity, or near unity, so that thermal accommodation has had a very small effect on drop growth or evaporation in the continuum.

The net kinetically evaluated thermal energy flux emanating from the surface of the drop is given by

$$\frac{\alpha}{4}\left[n(T_a)\bar{v}(T_a)\bar{\epsilon}_i(T_a) - n(T_d)\bar{v}(T_d)\bar{\epsilon}_s(T_d)\right].$$

(The total flux includes an additional term, $\frac{1}{2}k\partial T/\partial r$, as argued by Kennard 1938.) Here the first term denotes the incident flux, with $\bar{\epsilon}_i(T_a)$ the average energy associated with an effusing "beam" at temperature T_a, and the second term denotes the evaporative flux, evaluated at the drop temperature T_d, and equated to the incident flux that would ensure equilibrium conditions. The erroneous factor of two arises when the flux term, $n\bar{v}$, is evaluated at T_a and simply factored out of the above expression leaving the inconsistent result

$$\frac{\alpha}{4}n(T_a)\bar{v}(T_a)[\bar{\epsilon}_i(T_a) - \bar{\epsilon}_s(T_d)],$$

(i.e., the approximation $T_a \approx T_d$ has been applied only to the product $n\bar{v}$). A consistent result is obtained by simply not indulging in this factorization, but carrying through the calculation assuming that $T_d - T_d$ is sufficiently small to justify the approximation

$$\left(1 + \frac{T_d - T_a}{T_a}\right)^{1/2} \approx 1 + \frac{1}{2}\frac{T_d - T_a}{T_a}.$$

This leads straightforwardly to Eq. (5).

REFERENCES

Alofs, D., M. B. Trueblood, D. R. White and V. L. Behr, 1979: Nucleation experiments with monodisperse NaCl aerosols. *J. Appl. Meteor.*, **18**, 1106–1117.

Anderson, J. B., J. Hallett and M. Beesley, 1981: An extended classical solution of the droplet growth problem, NASA TM82392, Marshall Space Flight Center, NTIS N81-17383.

Baker, M. B., R. E. Breidenthal, T. W. Choularton and J. Latham, 1984: The effects of turbulent mixing in clouds. *J. Atmos. Sci.*, **41**, 229–304.

Barnes, G. T., 1978: Insoluble monolayers and the evaporation coefficient for water. *J. Colloid Interface Sci.*, **65**, 566–572.

Baumgardner, D., 1988: Cloud droplet growth in Hawaiian orographic clouds. Ph.D. dissertation, University of Wyoming.

Bigg, K., 1986: Discrepancy between observation and prediction of concentrations of cloud condensation nuclei. *Atmos. Res.*, **20**, 81–86.

Bird, R. B., W. E. Stewart and E. N. Lightfoot, 1960: *Transport Phenomena.* Wiley, 779 pp.

Blyth, A. M., and J. Latham, 1985: An airborne study of vertical structure and microphysical variability within a small cumulus. *Quart. J. Roy. Meteor. Soc.*, **10**, 773–792.

Bullrich, K., and G. Hanel, 1978: Effects of organic aerosol constituents on extinction and absorption coefficients and liquid water contents of fogs and clouds. *Pure Appl. Geophys.*, **116**, 293–301.

Cammenga, H. K., 1980: Evaporation mechanics of liquids. *Current Topics in Materials Science*, E. Kaldis, Ed., **5**, North-Holland.

Carstens, J., 1979: Drop growth in the atmosphere by condensation: Application to cloud physics. *Adv. Colloid Interface Sci.*, **10**, 285–314.

——, J. Podzimek and H. Andriambeloma, 1986: Assessment of the impact of insoluble and surface active pollutants on fog evolution. Preprints, *Conf. on Cloud Physics*, Snowmass, Amer. Meteor. Soc., 32–35.

Cerni, T. A., 1983: Determination of the size and concentration of cloud drops with an FSSP. *J. Climate Appl. Meteor.*, **22**, 1346–1355.

Chodes, N. J., J. Warner and A. Gagin, 1974: A determination of the condensation coefficient of water from the growth rate of small droplets. *J. Atmos. Sci.*, **31**, 1351–1357.

Davis, E. J., 1983: Transport phenomena with single aerosol particles. *Aerosol Sci.*, **2**, 121–129.

Derjaguin, B. V., V. A. Fedoseyev and L. A. Rosenzweig, 1966: Investigation of the adsorption of cetyl alcohol vapor and the effect of this phenomenon on the evaporation of water drops. *J. Colloid Interface Sci.*, **22**, 45–50.

——, L. F. Leonov, S. V. Mogilat and V. M. Borisova, 1982: Dependence of water condensation coefficient on degree of interface coverage by cetyl alcohol monolayer. *Kolln. Zh.*, **44**, 877–883.

——, Y. S. Kurghin, S. P. Bakanov, and K. M. Merzhanov, 1985: Influence of surfactant vapor on the spectrum of cloud drops forming in the process of condensation growth. *Langmuir*, **1**, 278–281.

Dickenson, E., 1978: A hard disk fluid model of monolayer permeation and evaporation resistance. *J. Colloid Interface Sci.*, **633**, 461–471.

Fitzgerald, J. W., 1970: A re-examination of the classical theory of the growth of a population of cloud droplets by condensation. Preprints, *Conference on Cloud Physics*, Ft. Collins, Amer. Meteor. Soc., 111–114.

Fletcher, N. H., 1962: *The Physics of Rain Clouds.* Cambridge, 386.

Fukuta, N., and L. A. Walter, 1970: Kinetics of hydrometeor growth from a vapor spherical model. *J. Atmos. Sci.*, **26**, 1160–1172.

Garnier, J. P., Ph. Ehrhard, and Ph. Mirabel, 1987: Water droplet growth study in a continuous flow diffusion cloud chamber. *Atmos. Res.*, **21**, 41–52.

Garrett, W. D., 1978: The impact of organic material on cloud and fog processes. *Pure Appl. Geophys.*, **116**, 316–334.

Gill, P. S., T. E. Graedel and C. J. Weschler, 1983: Organic films on atmospheric aerosol particles, fog droplets, cloud droplets, raindrops, and snowflakes. *Rev. Geophys. Space Phys.*, **21**, 903–920.

Graedel, T. E., and C. J. Weschler, 1981: Chemistry within aqueous atmospheric aerosols and raindrops. *Rev. Geophys. Space Phys.*, **19**, 505–539.

Hagen, D. E., 1979: A numerical cloud model for the support of laboratory experimentation. *J. Appl. Meteor.*, **18**, 1035–1043.

——, 1986: UMR cloud simulation studies of droplet growth: Investigation of the condensation coefficient. Preprints, *Conference on Cloud Physics*, Vol. 2, Snowmass, Amer. Meteor. Soc., 1–4.

——, D. R. White and D. J. Alofs, 1988: Condensation method for humidity measurement in the UMR cloud simulation chamber. *J. National Bureau of Standards*, **93**, 551–556.

Hickman, K., 1966: Reviewing the evaporation coefficient. *Desalinization*, **1**, 13–29.

Hoppel, W. A., Twomey, S. and T. A. Wojciechowski, 1979: A segmented thermal diffusion chamber for continuous measurement of CN. *J. Aerosol Sci.*, **10,** 369–373.

Jensen, J. B., and M. B. Baker, 1986: An observational study of cloud droplet spectra in continental cumulus clouds. Preprints, *Conference on Cloud Physics,* Vol. 2, Snowmass, Amer. Meteor. Soc., 145–148.

——, P. H. Austin, M. B. Baker and A. M. Blythe, 1985: Turbulent mixing, spectral evolution and dynamics in a warm cumulus cloud. *J. Atmos. Sci.*, **42,** 173–192.

Jonas, P. R., and B. J. Mason, 1982: Entrainment and the droplet spectrum in cumulus clouds. *Quart. J. Roy. Meteor. Soc.*, **108,** 857–869.

Kennard, E. H., 1938: *Kinetic Theory of Gases.* McGraw-Hill, 475 pp.

LaMer, V. K., 1962: *Retardation of Evaporation by Monolayers: Transport Processes.* Academic Press, 277 pp.

Lucassen-Reynders, E. H., and J. Lucassen, 1969: Properties of capillary waves. *Adv. Colloid Interface Sci.*, **2,** 347–395.

Maa, J. R., 1983: The role of interfaces in heat transfer processes. *Adv. Colloid Interface Sci.*, **18,** 227–280.

Manton, M. J., and J. Warner, 1982: On the droplet distribution near the base of cumulus clouds. *Quart. J. Roy. Meteor. Soc.*, **108,** 917–928.

Mason, B. J., and P. R. Jonas, 1974: The evolution of droplet spectra and large droplets by condensation in cumulus clouds. *Quart. J. Roy. Meteor. Soc.*, **100,** 23–38.

Mills, A. F., and R. A. Seban, 1967: The condensation coefficient of water. *Int. J. Heat Mass Transfer,* **10,** 1815–1827.

Mozurkewich, M., 1986: Aerosol growth and the condensation coefficient of water: A review. *Aerosol Sci.*, **3,** 177–185.

Narasawa, U., and G. S. Springer, 1975: Measurements of evaporation rates of water. *J. Colloid Interface Sci.*, **50,** 392–395.

Palmer, H. J., and A. Bose, 1981: Bulk phase and intrinsic interfacial resistance to evaporation under a vacuum. *J. Colloid Interface Sci.*, **84,** 291–300.

Paluch, I. R., and C. A. Knight, 1986: Does mixing promote cloud droplet growth?. *J. Atmos. Sci.*, **43,** 1994–1998.

——, and ——, 1987: Reply (to Telford). *J. Atmos. Sci.*, **44,** 2355–2356.

Pich, J., 1976: Theory of diffusive deposition of particles in a sphere and in a cylinder at small Fourier numbers. *Atmos. Environ.*, **10,** 131–135.

Plooster, M., 1979: Atmospheric cloud physics laboratory simulation system: Mathematical description. Rep. under NASA Contract NAS8-32688, General Electric Co. [Valley Forge Space Center, P.O. Box 8555, Philadelphia, PA 19101.]

Pruppacher, H. R., and J. D. Klett, 1978: *Microphysics of Clouds and Precipitation.* Reidel, 714 pp.

Radke, L., J. Lyons, D. Hegg, P. Hobbs, D. Sandberg and D. Ward, 1983: Airborne monitoring and smoke characterization of prescribed fires on forest lands in Western Washington and Oregon. Rep. EPA 600/X-83-047, EPA contract 68-03-3050, Lockheed Engineering and Management Services Co., Las Vegas.

Rubel, G. O., and J. W. Gentry, 1984: Measurements of the kinetics of solution droplets in the presence of adsorbed monolayers: Determination of water accommodation coefficients. *J. Phys. Chem.*, **88,** 3142–3148.

——, and ——, 1985: Measurement of water and ammonia accommodation coefficients at surfaces with adsorbed monolayers of hexadecanol. *J. Aerosol Sci.*, **16,** 571–574.

Sageev, G., R. E. Flagan, J. H. Seinfeld and S. Arnold, 1986: Condensation rate of water on aqueous droplets in the transition regime. *J. Colloid Interface Sci.*, **113,** 421–429.

Schmitt, J. L., 1981: Precision expansion cloud chamber for homogeneous nucleation studies. *Rev. Sci. Instrum.*, **52,** 1749–1754.

Schulze, F.-W., and H. K. Cammenga, 1980: Investigation of the phase transition kinetics liquid-vapor by a pressure-jump relaxation technique. *Ber. Bunsenges Phys. Chem.*, **84,** 163–168.

Sherwood, T. K., R. L. Pigford and C. R. Wilke, 1975: *Mass Transfer,* McGraw-Hill, 182 pp.

Telford, J., and S. K. Chai, 1980: A new aspect of condensation theory. *Pure Appl. Geophys.*, **118,** 720–742.

——, and P. B. Wagner, 1981: Observations of condensation growth determined by entity type mixing. *Pure Appl. Geophys.*, **119,** 934–965.

Toosi, R., and T. Novakov, 1984: The lifetime of aerosols in ambient air: Consideration of the effects of surfactants and chemical reactions. *Atmos. Environ.*, **18,** 1–7.

Wagner, P. E., 1982: Aerosol growth by condensation. *Topics in Current Physics, Aerosol Microphys II* W. H. Marlow, Ed., Springer-Verlag, 129–178.

Warner, J., 1969: The microstructure of cumulus cloud. Part II. The effect on droplet size distribution of the cloud nucleus spectrum and updraft velocity. *J. Atmos. Sci.*, **26,** 1272–1284.

White, D., J. L. Kassner, J. C. Carstens, D. E. Hagen, J. L. Schmitt, D. J. Alofs, A. R. Hopkins, M. B. Trueblood, M. W. Alcorn and W. L. Walker, 1987: University of Missouri—Rolla cloud simulation facility: Proto II chamber. *Rev. Sci. Instrum.*, **58,** 826–834.